Localizations on complex networks

Guimei Zhu,[1,2] Huijie Yang,[2,3] Chuanyang Yin,[1,2] and Baowen Li[2,4,*]
[1]*Department of Modern Physics, University of Science and Technology of China, Hefei Anhui 230026, China*
[2]*Department of Physics and Centre for Computational Science and Engineering, National University of Singapore, Singapore 117542, Republic of Singapore*
[3]*School of Management, Shanghai University for Science and Technology, Shanghai 200092, China*
[4]*NUS Graduate School for Integrative Sciences and Engineering, Singapore 117597, Republic of Singapore*
(Received 20 October 2007; revised manuscript received 18 February 2008; published 23 June 2008)

We study the structural characteristics of complex networks using the representative eigenvectors of the adjacent matrix. The probability distribution function of the components of the representative eigenvectors are proposed to describe the localization on networks where the Euclidean distance is invalid. Several quantities are used to describe the localization properties of the representative states, such as the participation ratio, the structural entropy, and the probability distribution function of the nearest neighbor level spacings for spectra of complex networks. Whole-cell networks in the real world and the Watts-Strogatz small-world and Barabasi-Albert scale-free networks are considered. The networks have nontrivial localization properties due to the nontrivial topological structures. It is found that the ascending-order-ranked series of the occurrence probabilities at the nodes behave generally multifractally. This characteristic can be used as a structural measure of complex networks.

DOI: 10.1103/PhysRevE.77.066113 PACS number(s): 89.75.Hc, 72.15.Rn, 05.50.+q, 05.45.Df

I. INTRODUCTION

Recent years have witnessed an avalanche of research on complex networks and their applications in diverse fields [1]. Structural measures of complex networks are the cornerstone for understanding the relations between structures, dynamics, and functions. Real-world networks generally have nontrivial properties, such as the small-world [2], scale-free [3], motif [4], modularity, hierarchy [5], and fractal [6] properties, and so on. The small-world effect is that on average the nodes can reach each other with only a small number of hops. The scale-free property refers to the number of edges per node obeying a right-skewed distribution. It is also found that some special subgraphs containing several connected nodes, called motifs, occur with significant probabilities compared with those in the corresponding randomized networks. These three individual, paired, or local-pattern-based properties are called microproperties. On the other hand, modularity is a kind of macroproperty representing that a network can be separated into loosely connected groups within which the nodes are densely connected.

To a certain degree, dynamics on networks can be regarded as the transport processes of mass, energy, signal, and/or information at different structural scales [7,8]. Sometimes we have to deal with networks with an unreasonably large number of nodes and edges, e.g., neuron networks and the worldwide web, when designing a coarse-graining procedure is essential [9]. The patterns at different scales may provide a reasonable solution to these problems. It is found that some real-world networks have hierarchical structures, in which the small-world and scale-free properties can coexist [5]. Moreover, many real-world networks behave self-similarly at different structural levels (fractal behavior) [6].

Although great progress has been achieved, the measures of complex networks are not yet fully understood. Just as pointed out by Newman [10], our techniques for analyzing networks are at present no more than a grab-bag of miscellaneous and largely unrelated tools, and we still do not have a systematic program for characterizing network structures. Furthermore, the measures of network structures, such as the microproperties, the patterns at different scales, and the macroproperties, are generally simple applications of the concepts in graph theory, bioinformatics, social science, and fractal theory, namely, they are not dynamics based. We cannot expect simple and reasonable relations between the measures and the dynamical processes on networks.

The lack of powerful tools to characterize network structures is an essential bottleneck in understanding dynamical processes on networks. One typical example is the synchronizability of complex networks. Detailed work shows that almost all the structural measures affect the synchronizabilities in complicated ways [11], based upon which we cannot reach a clear picture of the mechanisms for synchronization processes on networks.

Dynamics-based measures of complex networks may be the key to the problems. The structures of complex networks can induce nontrivial properties in the physical processes occurring on them. The physical processes in turn can be used as a probe to capture the structural properties. Well-studied dynamical processes, such as random walks [12,13] and Boolean dynamics [14], can be good candidates as probes. To cite an example, random walks on complex networks that are biased toward a target node show a localization-delocalization transition [12].

In the present paper, we map networks to large clusters, namely, the nodes and edges to atoms and the bonds between them, respectively. The localization properties of electrons in the clusters can be used as measures of the structural properties of the networks. We try to detect global symmetries from the spectra and the eigenvectors of complex networks.

*phylibw@nus.edu.sg

Very recently, much attention has been focused on detecting global characteristics embedded in spectra of complex networks due to their potential application in understanding the organization mechanisms and the synchronization dynamics of complex networks [8,15,16]. To our best knowledge, this is the first time that the global characteristics of complex networks have been detected from the eigenvectors, which contain more information about the system than eigenvalues.

In addition to being a measure of network structures, the structure-induced localization may have potential applications in understanding the electronic properties of materials such as conductive polymers and carbon nanonets. The intrachain windings in conductive polymers can introduce long-range edges into the original one-dimensional systems, resulting in nontrivial network structures [17,18]. It is also found that random networks of carbon nanotubes, called nanonets, can mimic a variety of basic electronic functions from the conductive properties of metals to the less conductive characteristics of semiconductors [19]. Indeed, nanonets have paved the way for carbon to serve as the foundation for future electronic devices. The effect of network structures on electronic properties has been one of the most active topics in recent years [7,20].

The paper is organized as follows. In Sec. II the concept of localization on complex networks is presented. The occurrence probabilities on the nodes are proposed to describe quantitatively the localization effects. In Sec. III the methods to measure the localization properties are described in detail. The participation ratio, the structural entropy, and the probability distribution function of the nearest neighbor level spacings of spectra are used to illustrate the localization in a global way. Wavelet transform is then used to find the detailed structural properties of the probability distribution function of the occurrence probabilities on the nodes. As examples, we consider the Watts Strogatz small-world and the Barabasi-Albert scale-free model networks and whole-cell networks in the real world. The results are shown in Sec. IV. We will show that the global symmetries in networks can induce multifractal structures in the eigenvectors. As a conclusion, the nontrivial structures of complex networks can induce significant localization, which in turn can be used as a global measure of the structural symmetries.

II. LOCALIZATIONS ON NETWORKS

We consider an undirected complex network with N identical nodes, whose topological structure can be described by an adjacency matrix A. The elements A_{ij} are 1 (0) if the nodes i and j are connected (disconnected), respectively. If we consider the nodes as atoms and the edges as bonds, the network can be mapped to a large molecule [16]. For an electron moving in such a molecule, the tight-binding Hamiltonian is

$$\mathcal{H} = \sum_{n=1}^{N} \varepsilon_n |n\rangle\langle n| + \sum_{m \neq n}^{N} A_{mn} t_{mn} |m\rangle\langle n|, \tag{1}$$

where ε_n is the site energy and $t_{mn}A_{mn}$ the hopping integral for the bond between sites m and n.

The tight-binding Hamiltonian Eq. (1) is usually used to study disorder-induced localizations. In the present form, the matrix A is explicitly introduced to describe the structure of the system. For a one-dimensional perfectly regular lattice, we have $\varepsilon_n = \varepsilon$, $t_{mn} = t$, and $A_{mn} = \delta(m-n \pm 1)$. The Bloch wave function of an electron extends all over this perfectly regular lattice. Disorder in structures can induce a transition from extended to localized states. The wave function for a localized state decreases exponentially with the distance from its center. The disorder effects include random distributions of the site energies (ε_n), the hopping integrals (t_{mn}), and the edges in the structures (A_{mn}). The disorder comes from the different kinds of atoms on the lattice points, differences of the separations of successive lattice points, and randomness in the structure. At the same time, there may be some symmetries in the distributions of the site energies, the hopping integrals, and the edges, which may lead to delocalization of the wave functions.

In the usual Anderson model [21], the disorder effect due to the random distribution of the site energies is considered, i.e., ε_n is a random variable satisfying a certain distribution probability function while $t_{mn} = t$, $A_{mn} = \delta(m-n \pm 1)$. The site energies may obey a special distribution rather than that in the Anderson model, such as a periodic [22] or a power-law [23] function. In the literature [24,25], a one-dimensional quasicrystal model has been introduced that the separation of two successive lattice points takes one of the two values u and v. This model considers the disorder effect of the distribution of the hopping integrals. We have $\varepsilon_n = \text{const}$, $t_{mn} = t_u$ or t_v, and $A_{mn} = \delta(m-n \pm 1)$. t_u and t_v are the hopping integrals corresponding to the separations u and v, respectively. It is found that quantum systems with quasiperiodic structures are in an intermediate state, which can be described with critical wave functions. A critical wave function obeys a power law with respect to the distance from its center.

To investigate problems such as vibrational spectra of glasses, instantaneous normal modes in liquids, electron hopping in amorphous semiconductors, and combinatorial optimization, Euclidean random matrix models are widely used in the literature [26], in which the disorder is due to the random positions of the sites, and the matrix elements are given by a deterministic function of the distances.

The models mentioned above generally focus on the disorder effects of the site energies and the hopping integrals. These models have also been extended to nontrivial structured systems such as the Cayley tree [27] and small-world networks [17]. Nontrivial effects of the structures of the systems are reported, but the interplay between the disorder due to the site energies and that due to the structures makes it difficult to distinguish the structure disorder effect from the site energy disorder effect.

In the networks considered in the present paper, however, the nodes are all identical and the disorder effect comes from the nontrivial topological structure. We focus our attention on the disorder effect of the network structure, that is, we assign $\varepsilon_n = 0$ and $t_{mn} = 1$, which leads to $H = A$. The localization on the network refers to the network structure-induced characteristics of the wave functions for this system. The usual Anderson model [21] is a special case where there exist

connections in the networks only between the nearest neighbors in Euclidean space.

Statistically, the structures of networks should display certain symmetries due to the general rules obeyed in the construction of the networks. Recent work demonstrated that many theoretical and real-world networks have statistically self-similar structures [6]. Therefore, there are two competitive mechanisms determining the wave function properties: the randomness of the bonds in the networks tends to cause localization of the wave function, whereas the symmetries of the networks tend to make the wave function extended. We thus expect rich structures embedded in the wave functions. As is well known, aperiodic crystals lead to fractal wave functions [25,28]. An interesting question is then how the global symmetries of networks affect the localization properties. The localization can be used as a probe of the characteristics of the network structures.

The states in the center of the energy band have the best chance to remain extended for a moderately disordered system. The eigenvector corresponding to the special eigenvalue close to the center of the spectrum for a network, denoted by E_c, is employed as the representative state to illustrate the characteristics of the considered system.

In the traditional study of wave function localization, the physical systems have deterministic structures in real-world Euclidean space, which leads to natural definitions of the localized, intermediate, and extended states of the systems. Obviously, these definitions are invalid for general complex networks without deterministic structures in Euclidean space. In this paper, we describe the localization effects using the probability distribution function (PDF) of the occurrence probabilities at the nodes, i.e., the values of the components for the representative eigenvector. Based on the PDF of the occurrence probabilities, the traditional definitions are extended to a much more general version to describe the localization properties on complex networks.

In Euclidean space, for a state $\Psi(r)$, the occurrence probability is $\rho(r)=|\Psi(r)|^2 \equiv F(r)$. Because the value of the distance r is distributed homogeneously in the considered region, we can regard it as a homogeneously distributed random variable. The direct sampling method in Monte Carlo simulations tells us that the probability distribution of ρ should be $P(\rho) \propto \frac{dF^{-1}(\rho)}{d\rho}$. Hence, it is reasonable to define the localized, critical, and perfectly extended states on complex networks using the PDFs of the occurrence probabilities,

$$P(\rho) \propto \begin{cases} \delta(\rho-\rho_0), & \text{extended}, \\ \rho^{-(1+\eta)} \mid \eta > 0\,, & \text{critical}, \\ \rho^{-(1+\eta)} \mid \eta = 0\,, & \text{localized}. \end{cases} \tag{2}$$

The PDF of the representative function is a very powerful measure for capturing the localization properties. It can be used to find the localization properties without using the distance in real-world Euclidean space.

Because no derivative exists for a fractal wave function in Euclidean space, the extension procedure in defining critical and localized states on networks cannot be simply used to define fractal properties on networks by using the PDF of the occurrence probabilities. In the present paper, we detect directly the fractal characteristics in the ascending-order-ranked series of the the occurrence probabilities, as described in detail in Sec. III C.

III. METHODS

A. Structural entropy

We denote the representative state as $V=(V_1, V_2, \ldots, V_N)$. The occurrence probabilities at the nodes are $\rho_m=|V_m|^2$, $m=1,2,\ldots,N$. The localization extent of the state can be described quantitatively with the participation ratio [29,30],

$$Q = \frac{1}{N \sum_{m=1} \rho_m^2}. \tag{3}$$

For a perfect extended state we have $Q=1$, while for a state strongly localized on one node it tends to $\frac{1}{N}$. Generally, Q should be in the range of $[\frac{1}{N}, 1]$.

However, this participation ratio can capture only the primary-level complexity in the localization properties, namely, the extension of the representative eigenvector to NQ nodes on the network. Many PDFs with different localization behaviors may result in the same Q. The simplest one is a steplike function: on NQ nodes the occurrence probabilities are $\frac{1}{NQ}$, while on the left $N(1-Q)$ nodes the occurrence probabilities are 0.

The secondary-level complexity in the localization properties is the deviation of the PDF from the steplike function. This deviation corresponds to the shape of the PDF, which can be extracted by using the structural entropy [31]

$$S_{\text{str}} = -\sum_{m=1}^{N} \rho_m \ln \rho_m - \ln(QN). \tag{4}$$

For the simple steplike condition, we have $S_{\text{str}}=0$. $S_{\text{str}} \neq 0$ tells us the shape deviation of PDF from the simple one. The pair of localization quantities (Q, S_{str}) is widely used up to date to describe the localization in disordered and aperiodic systems, and for the statistical analysis of spectra in diverse fields such as quantum chemistry, condensed matter physics, and quantum chaos [32,33].

B. Statistical properties of the spectra

The localization property can also be described with the random matrix theory (RMT) [30,34–36]. RMT was initially developed to understand the energy levels of complex nuclei and other kinds of complex quantum systems. Recently, the RMT theory has been proposed to capture the structural and dynamical properties of complex networks [15].

One of the most important quantities in the theory is the PDF for the nearest neighbor level spacing (NNLS) of the spectrum. It is theoretically and numerically confirmed that in the localized and extended states the PDFs of the NNLS should be the Poisson and Wigner-Dyson distributions, respectively [37–39]. Generally, for an intermediate state, the PDF obeys the Brody distribution

$$U(s) = \frac{\beta}{\xi} s^{\beta-1} \exp\left[-\left(\frac{s}{\xi}\right)^{\beta}\right], \tag{5}$$

where s is the NNLS and ξ the characteristic distribution width. The Poisson and the Wigner-Dyson distributions are the two extremes with $\beta=1$ and 2, respectively.

Introducing the accumulated function $C(s)=\int_0^s U(x)dx$, some trivial calculations lead to

$$\ln R(s) \equiv \ln\left[\ln\left(\frac{1}{1-C(s)}\right)\right] = \beta \ln s - \beta \ln \xi. \tag{6}$$

From this formula we can determine reliably the values of the parameters β and ξ.

To obtain the spacing s in units of the local mean level spacing, we should conduct a standard procedure, called unfolding. Denoting the spectrum of a network by $\lambda_1, \lambda_2, \ldots, \lambda_N$, the accumulation density function for the spectrum is $G(\lambda_m)=m$, $m=1,2,\ldots,N$. Fitting this relation with a polynomial function, we can separate it into a smooth part and a fluctuating part as

$$G(\lambda_m) = G_{av}(\lambda_m) + G_f(\lambda_m). \tag{7}$$

The NNLS can be obtained as $P(\rho) \sim \rho^{-(1+\eta)}$. For a complex network, we generally have not enough knowledge of its spectrum, and the polynomial function fitting method can lead to a reliable result. In this paper, the order of the polynomial function is 17.

C. Wavelet transform

The detailed properties for the PDF of the occurrence probabilities can be used as a measure of the global structural symmetries. However, determining this PDF is a nontrivial task [40]. Assume the probability values have been sorted in ascending order, namely, $\rho=\{\rho_1 \le \rho_2 \cdots \le \rho_N\}$, which can be regarded as the profile of the nearest spacing series, $\Delta\rho = \{\rho_2 - \rho_1, \rho_3 - \rho_2, \cdots, \rho_N - \rho_{N-1}\}$. The local structures of $\Delta\rho$ can tell us the probability distribution function of ρ. It is found that the series ρ generally behaves multifractally.

The wavelet transform (WT) [41] is used to detect the fractal properties embedded in the ascending-order-ranked series ρ. The increasing trend in the series ρ makes box-counting-based techniques invalid to quantify the local scalings. In the wavelet transform, the contributions of the polynomial trends can be removed effectively. A multifractal series can be decomposed into many subsets characterized by different local Hurst exponent h, which quantifies the local singular behavior and thus is related to the local scaling of the series. The statistical properties of these subsets can be quantified by the fractal dimension $D(h)$ of the subset whose local Hurst exponent is h.

As a standard procedure, we first find the WT maximal values $\{T_g(a,\rho_k(a))|k=k_1,k_2,\ldots,k_J\}$, where a is the given scale. The partition function should scale in the limit of small scales as

$$Z(a,q) = \sum_{k=k_1}^{k_J} |T_g(a,\rho_k(a))|^q \sim a^{\tau(q)}. \tag{8}$$

The fractal dimension $D(h)$ can be obtained through the Legendre transform,

$$D(h) = qh - \tau(q), \quad h = \frac{d\tau(q)}{dq}. \tag{9}$$

For a monofractal structure we have a linear relation $\tau(q) = qH - 1$. H is the global Hurst exponent. For positive and negative q, $\tau(q)$ reflects the scaling of the large fluctuations and small fluctuations, respectively.

We use the real analytical wavelet $g^{(n)}$ among the class of derivatives of the Gaussian function, by which the polynomial trends up to order n can be removed. The results with $n=7$ are presented. $n=5$ and 6 lead to almost the same results. As comparison, we detect also the scaling behaviors in the randomized series ρ_R, called the shuffled series.

In this paper, we are interested in the characteristic point at which the fractal dimension reaches its maximum value $(h_c, D(h_c))$. It can tell us the nonhomogeneous distribution of the series ρ and the fractal characteristics of the principal subset.

IV. NUMERICAL RESULTS

We examine the localization behaviors for cellular networks [42], which are compiled by using a graph-theoretical representation of all the biochemical pathways based upon the WIT integrated-pathway genome database of 43 species from Archaea, Bacteria, and Eukarya [43]. The WIT (What Is There) is a system designed to support comparative analysis of sequenced genomes and generate metabolic reconstructions based upon chromosomal sequences and metabolic modules. Whole-cell networks consider cellular functions such as intermediate metabolism and bioenergetics, information pathways, electron transport, and transmembrane transport. The directed edges are replaced simply with nondirected edges. We consider only cellular networks with sizes larger than 500.

We study also the localization behaviors for the Watts-Strogatz small-world (WSSW) [2] and the Barabasi-Albert scale-free (BASF) [3] networks. For the WSSW model, we construct first a regular circular lattice with each node connecting with its d right-handed nearest neighbors. For each edge we rewire it with probability p_r to another randomly selected node. Self- and double edges are forbidden. In this way, we can introduce randomness into the resulting networks. Moreover, compared with the initial regular lattice, the rewiring procedure may introduce also "long-range" edges to the resulting networks, which can reduce significantly the average number of hops required for the nodes to reach each other. This is the so-called small-world effect.

The BASF networks are the results of a preferential growth mechanism, which exists widely in diverse fields. Starting from several connected nodes as a seed, at each growth step a new node is added and w edges are established between this node and the existing network. The probability

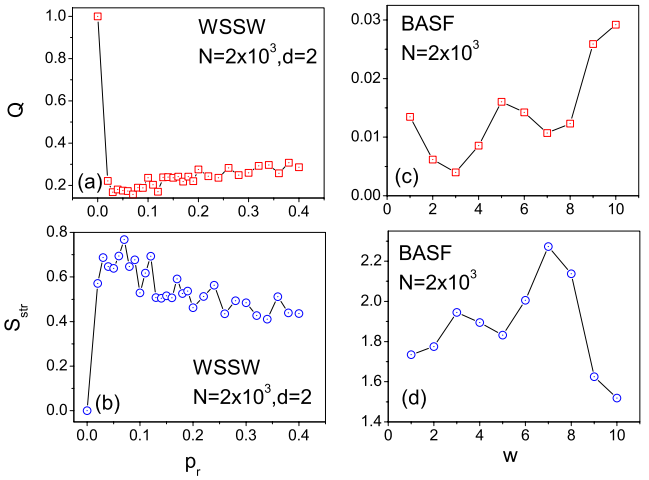

FIG. 1. (Color online) Localization quantities (Q, S_{str}) for the WSSW and BASF networks. There exist complex relations between p_r or w and (Q, S_{str}) for the BASF and WSSW networks. For the WSSW networks, from $p_r=0$ to $p_r=0.02$ there exists an abrupt decrease or increase in the value of (Q, S_{str}), as shown in (a) and (b), respectively. Then with increase of the rewiring probability p_r, the participation ratio tends to increase while the structural entropy tends to decrease. (c), (d) Results for BASF networks.

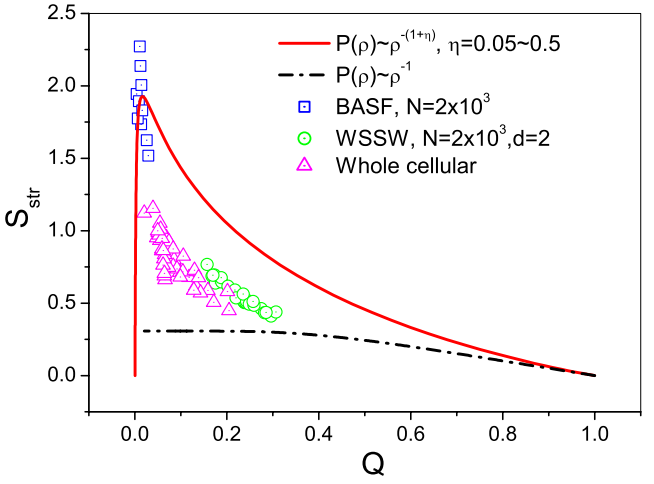

FIG. 2. (Color online) Relations of S_{str} versus Q for the WSSW, BASF, and whole-cell networks. The localization quantities for the distributions $P(\rho) \sim \rho^{-(1+\eta)}$ and $P(\rho) \sim 1/\rho$, namely, the critical and localized states, are shown as references. Starting from $\rho(r) \sim r^{-\sigma}$, the set of normalized values of $\rho(n/N)$, $n=1,2,\ldots,N$ can be regarded as the critical state. Assigning $\sigma=1-10$, the corresponding values of η are 0.5–0.05. N is the size of the considered network. The same procedure is also used to generate the localized states by starting from $\rho(r) \sim \exp(-\mu r)$. The localized states with $\mu=0.01-100$ are generated. The localization properties of the BASF networks can be captured by the critical state with extremely small values of η. The WSSW and whole-cell networks are generally in between the two typical states.

for an existing node to be connected with the new node is proportional to its degree. Self- and double edges are forbidden. For the resulting networks, the number of edges per node obeys a power law, namely, no characteristic scale exists in this distribution.

Figure 1 presents the localization quantities (Q, S_{str}) for the networks. For the WSSW networks, the randomness introduced by the rewiring procedure has two competing effects, the long-range edges which favor extension, and the breaking of symmetry which induces localization. For the BASF networks, the increase of w increases the heterogeneity and the connections between the nodes, which induce localization and extension, respectively. Hence, there exist complex relations between p_r or w and (Q, S_{str}) for the two kinds of networks, as shown in Figs. 1(a) and 1(b) and 1(c) and 1(d), respectively. For the WSSW networks, the participation ratio decreases rapidly from 1 to 0.22 when p_r changes slightly from 0 to 0.02, and then goes up gradually with the increase of p_r. As for the structural entropy, it increases abruptly when p_r changes from 0 to 0.02; after that it decreases gradually with increase of p_r.

Figure 2 shows S_{str} versus Q. As references, we calculate also the localization quantities for the critical and the localized states, namely, $P(\rho) \sim \rho^{-(1+\eta)}$ and $P(\rho) \sim \frac{1}{\rho}$, respectively. Starting from $\rho(r) \sim r^{-\sigma}$, we calculate the values of $\rho(\frac{n}{N})$, $n=1,2,\ldots,N$. The resulting normalized values can be regarded as the localized state. The critical states with $\sigma=1-10$ are calculated, and the corresponding values of η are 0.5–0.05, respectively. N is the size of the considered network. The same procedure can be used to generate the localized states by starting from $\rho(r) \sim \exp(-\mu r)$. The localized states with $\mu=0.01-100$ are generated.

The localization properties of the BASF networks can be captured by the critical states with extremely small values of η. The WSSW and whole-cell networks are generally in between the two typical (localized and extended) states.

We find that the PDFs of the NNLSs for all the networks can be described very well by using the Brody distribution in a unified way. The results for the parameter β are shown in Fig. 3. For WSSW networks, with the increase of the rewiring probability p_r, the parameter β increases rapidly from 1.02 ± 0.053 at $p_r=0$ to 1.95 ± 0.065 at $p_r=0.14$. For $p_r > 0.14$, β is almost the same, namely, ~ 2.0. That is, the

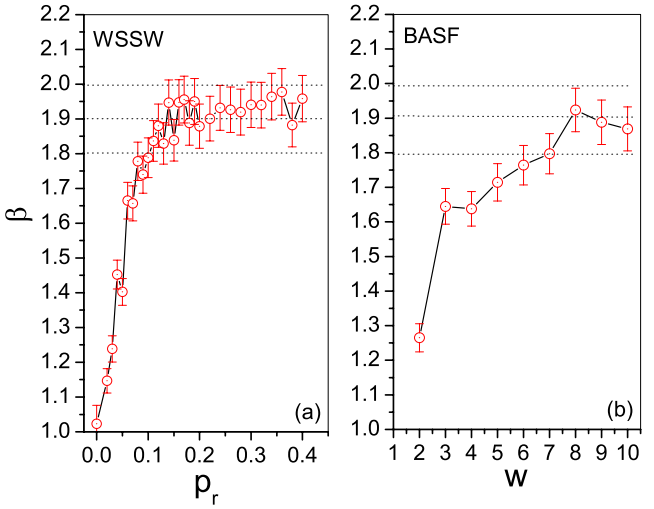

FIG. 3. (Color online) Value of Brody parameter β versus network parameters p_r and w. (a) WSSW and (b) BASF networks.

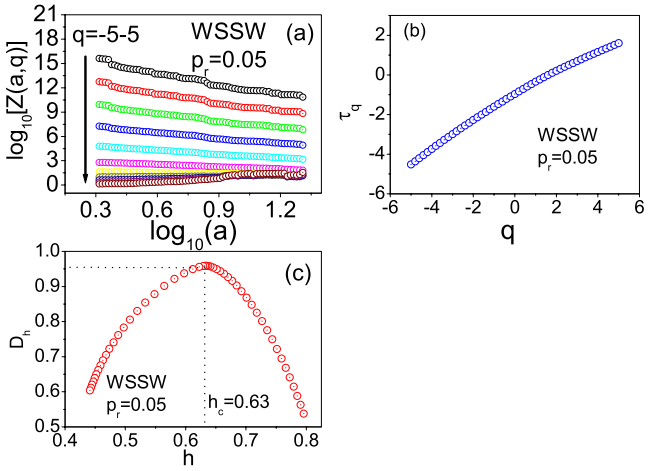

FIG. 4. (Color online) Multifractal scaling characteristics of the ascending-order-ranked series ρ for the real-world, WSSW, and BASF networks. The multifractal behavior for the WSSW network with $d=2$, $N=2000$, and $p_r=0.05$ is presented as a typical example. In the whole range of $q=-5$ to 5, there is only one characteristic point $(h_c, D(h_c))=(0.63, 0.958)$.

representative eigenvector changes from a nearly localized state ($p_r=0$) to an extended state in this interval of p_r. For networks with $p_r>0.14$, the representative eigenvectors are almost perfectly extended, while for BASF networks, with increase of w, the greater number of edges can induce significant extensions of the representative states. β reaches its asymptotic value ~ 1.90. Due to the heterogeneity, BASF networks cannot reach a perfectly extended state.

In a considerably wide range of q, the partition functions behave scale-invariantly as in Eq. (8). There are three kinds of typical WT transform results. Here we present several typical examples. In the whole range of $q=-5$ to 5, the WSSW network with $p_r=0.05$ and the BASF network with $w=8$ are multifractal with only one characteristic point $(h_c, D(h_c))$, as shown in Figs. 4 and 5, respectively. Sometimes, the multifractal degenerates to a monofractal. Figure 6 gives another condition where the fractal behaviors can be separated into two branches, namely, $q<0$ and $q>0$. The characteristic points for these two branches are not the same. That is, the principal subsets for the large and the small fluctuations are different. These three conditions are called monofractal, multifractal, and branched multifractal, respectively.

The scaling properties for the real-world and model networks are listed in Table I. For the mono- and multifractals, we present simply the global Hurst exponent H and the characteristic point $(h_c, D(h_c))$, respectively. For the branched multifractal we give the scaling characteristics for the two branches $q<0$ and $q>0$, separated by the solidus /. To cite an example, for the cellular network *M. jannaschii*, the characteristic point for the branch $q<0$ is (0.63,0.96) and that for the branch $q>0$ is (0.83,1.03). It is denoted as (0.63,0.96)/(0.83,1.03). The results for the corresponding shuffled series are presented also. We discard the networks where the scaling behaviors of the original ρ and the randomized series ρ_R are undistinguishable. The sizes of the WSSW and BASF networks are $N=2000$. $N=1000$, 3000, and 4000 lead to almost same results (not shown in Table I).

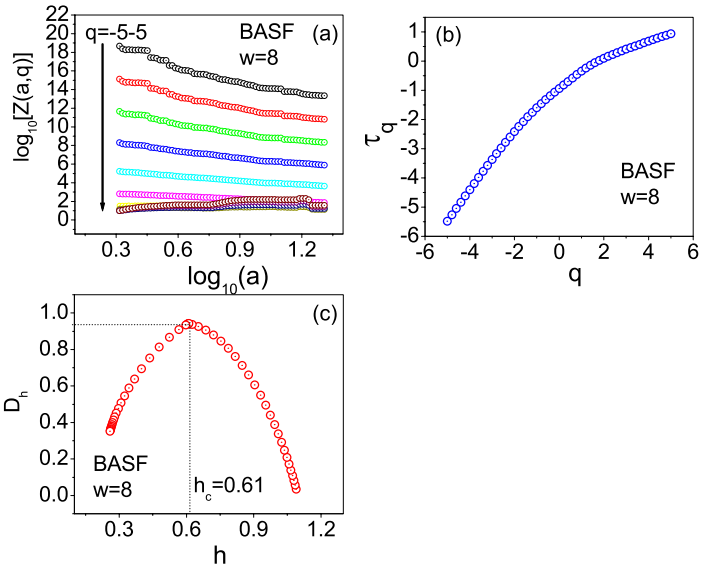

FIG. 5. (Color online) Multifractal scaling characteristics of the ascending-order-ranked series ρ for the real world, WSSW, and BASF networks. The multifractal behavior for the BASF network with $w=8$ and $N=2000$ is presented as a typical example. In the whole range of $q=-5$ to 5, there is only one characteristic point $(h_c, D(h_c))=(0.61, 0.942)$.

The WSSW and BASF networks are almost all mono- or multifractals with the values of h_c mainly in the range of 0.66 ± 0.05. However, most of the considered real-world networks behave as branched multifractals. Hurst exponents larger than 1 and near 0 correspond to nonsingularity and white noise, respectively. Discarding these trivial conditions, we find that the multifractal behaviors are embedded in the branches of $q>0$, and the values of h_c are basically in the range of 0.8 ± 0.05. The larger values of h_c for the large

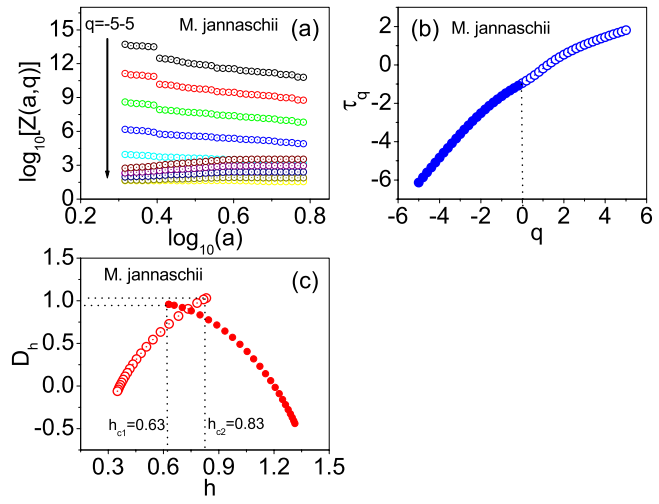

FIG. 6. (Color online) Branched multifractal scaling characteristics of the ascending-order-ranked series ρ for the real-world and model networks. The branched multifractal behavior for the whole-cell network of *M. jannaschii* is presented as a typical example. The two branches $q<0$ and $q>0$ lead to different characteristic points $(h_{c1}, D(h_{c1}))=(0.63, 0.96)$ and $(h_{c2}, D(h_{c2}))=(0.83, 1.03)$.

TABLE I. The scaling properties of the ascending-order-ranked series ρ for the WSSW, BASF, and whole-cell networks. The characteristic points $(h_c, D(h_c))$ for multifractals or H for monofractals are presented, which reflect the characteristics of the principal subsets. For the branched multifractals, the characteristic points for the branches $q>0$ and $q<0$ are separated by the solidus /. The results for the shuffled series are also presented as comparison. h_c for the WSSW and BASF networks is basically in the range of 0.66 ± 0.05, while that for the whole-cell networks is much larger, 0.8 ± 0.05. The asterisks denote the absence of the corresponding branches.

Networks		Original series $H, H_1, H_2, (h_c, D(h_c))$	Shuffled series H, H_1, H_2, H, H_1, H_2	Networks		Original series $H, H_1, H_2, (h_c, D(h_c))$	Shuffled series $H, H_1, H_2, (h_c, D(h_c))$
Cellular [3]	*M. jannaschii*	(0.63, 0.96) / (0.83, 1.03)	** /(0.42, 0.869)	Cellular [3]	*S. pneumoniae*	0.40	** /(0.60, 0.908)
	A. aeolicus	0.00/(0.61, 0.94)	(0.45, 0.877)		*M. thermo-autotrophicum*	0.72	(0.48, 0.863)
	B. subtilis	3.25/(0.81, 0.95)	(0.72, 0.924)		*T. maritime*	0.33	** /(0.66, 0.879)
	C. acetobutylicum	2.40/(0.88, 0.99)	** /(0.48, 0.922)	WSSW	$p_r=0.02$	(0.64, 0.980)	(0.35, 0.964)
	C. jejuni	0.07/(0.82, 0.95)	(0.71, 0.883)		$p_r=0.06$	(0.64, 0.959)	(0.43, 0.966)
	E. coli	1.45/(0.78, 0.95)	(0.45, 0.974)/ (0.68, 0.934)		$p_r=0.10$	(0.62, 1.004)	(0.34, 0.963)
	M. bovis	2.82/(0.85, 0.88)	(0.42, 0.889)		$p_r=0.14$	(0.68, 0.956)	(0.33, 0.963)
	M. tuberculosis	4.04/(0.75, 0.98)	(0.68, 0.936)		$p_r=0.18$	(0.64, 0.989)	(0.34, 0.964)
	N. meningitidis	0.22/(1.20, 1.06)	(0.76, 0.907)		$p_r=0.24$	1.000	(0.32, 0.967)
	S. cerevisiae	2.54/(0.89, 0.92)	** /(0.61, 0.889)		$p_r=0.28$	0.714	(0.32, 0.964)
	A. fulgidus	0.95/1.23	** /(0.57, 0.903)		$p_r=0.32$	(0.61, 0.967)	(0.27, 0.963)
	C. elegans	5.70/0.71	** /(0.50, 0.897)		$p_r=0.36$	0.687	(0.33, 0.962)
	C. tepidum	1.97/0.20	(0.49, 0.928)		$p_r=0.40$	0.546	(0.28, 0.961)
	D. radiodurans	2.82/1.14	(0.75, 0.964)	BASF	$w=1$	1.099	(0.887, 0.00)
	H. influenzae	3.82/0.59	(0.81, 0.964)		$w=2$	(0.58, 0.976)	(1.500/0.00)
	H. pylori	4.33/0.81	(0.61, 0.895)		$w=3$	0.638	1.135/0.00
	M. leprae	3.68/0.50	(0.70, 0.887)		$w=4$	1.06/0.40	1.197/0.00
	N. gonorrheae	2.84/1.13	(0.60, 0.923)		$w=5$	1.15/0.63	0.901/0.00
	P. gingivalis	3.44/0.63	** /(0.41, 0.912)		$w=6$	(0.64, 0.961)	0.847/0.00
	R. capsulatus	1.59/0.00	** /(0.68, 0.902)		$w=7$	(0.72, 1.014)	0.838/0.00
	P. aeruginosa	0.14/0.57	(0.68, 0.915)		$w=8$	(0.61, 0.942)	0.828/0.00
	A. antinomy-cetemcomitans	(0.54, 0.924)	(0.45, 0.901)		$w=9$	0.516	0.691/0.00
	E. faecalis	(0.84, 0.954)	(0.65, 0.880)		$w=10$	0.721	0.696/0.00

fluctuations in the real-world networks show us the much more nonhomogeneous structures of the PDFs of ρ. That is, the PDFs of ρ for real-world networks tend to form much sharper peaks at different scales.

It should be noted that in the present paper the structure-induced localization is used as a probe of structure properties of complex networks. We detect the localization properties for the WSSW and BASF model networks and the cellular networks, but it does not imply and require any localization-related dynamical process (such as waves) occurring in the real-world systems.

V. CONCLUSIONS

In summary, the probability distribution function of the representative eigenvector is proposed to describe the localization properties of complex networks. The localization quantities (Q, S_{str}), the PDFs of the NNLS, and the wavelet transform are used to capture the characteristics of the representative state. The nontrivial structures of the networks can induce localization of the representative states. At the same time, because of the global symmetries of the networks, the representative states have nontrivial structures rather than the steplike distribution.

The localization quantities (Q,S_{str}) and Brody distribution parameter β can describe the nontrivial localization properties in a global way. The (Q,S_{str}) values tell us that the BASF networks with $w=2$ are significantly localized compared with the WSSW networks with $d=2$. It is consistent with the conclusions drawn from the results of β. The whole-cell networks have localization properties much closer to those of the WSSW networks.

The wavelet transform can tell us details of the nontrivial structures of the representative eigenvectors. The ascending-order-ranked series ρ for the WSSW and BASF model networks and the whole-cell networks behave as monofractals, multifractals, or branched multifractals. The PDF of ρ tends to form sharp peaks at different scales in a self-similar way.

This kind of property can shed light on the global symmetries due to the general rules in the construction of the networks. Hence, it can be employed as a global measure of the network structure. Moreover, the structure-induced localizations on networks maybe helpful to understand the electronic conduction and heat transport properties [44] of nanonet materials.

A closely relevant topic is the diffusion on complex networks. Kim *et al.* [45] reported their work on quantum and classical diffusion on WSSW networks. The Hamiltonian is the same as that in the present paper, namely, $\varepsilon_n=0$ and $t_{mn}=1$ in Eq. (1). An electron is localized at a randomly selected node at the beginning, then the diffusion process is obtained by solving the time-dependent Schrödinger equation. It is found that the long-range edges can speed up diffusion significantly, especially at the transition point from $p_r=0$ to $p_r\neq 0$. This is qualitatively inconsistent with our findings of the significant changes of the participation ratio and the structural entropy (Q,S_{str}), when p_r increases from $p_r=0$ to 0.02.

As for the classical diffusion on networks, a very recent work reports the first-passage times of random walkers in complex scale-invariant media [13,46]. Many real-world networks have self-similar structures, and diffusion on networks can be regarded to a certain degree as diffusion on fractal media, which has attracted intensive attention for its importance in theories and potential use in diverse research fields [47].

However, we shoud point out that it is not trivial to compare our results quantitatively with these evolutionary processes. Actually our results are obtained from the eigenstates in energy representation, while for quantum diffusion the initial state of localization at a randomly selected node is a wave packet and the final state should be a superposition of the eigenstates in energy representation. How to relate the localization to the classical diffusion is definitely interesting but not a trivial task. Obviously, detailed work on diffusion on complex networks is required to understand the relation between localization and diffusion on networks.

ACKNOWLEDGMENTS

The work was supported by NUS Faculty Research Grant No. R-144-000-165-112/101. It is also supported by the National Science Foundation of China under Grant Nos. 70571074 and 106 35040. H.Y. gratefully acknowledges the support of the K. C. Wong Education Foundation, Hong Kong.

[1] D. J. Watts, *Small Worlds* (Princeton University Press, Princeton, NJ, 1999); R. Albert and A.-L. Barabasi, Rev. Mod. Phys. **74**, 47 (2002); S. N. Dorogovtsev and J. F. F. Mendes, *Evolution of Networks* (Oxford University Press, New York, 2003).
[2] D. J. Watts and S. H. Strogatz, Nature (London) **393**, 440 (1998).
[3] A.-L. Barabasi and R. Albert, Science **286**, 509 (1999).
[4] R. Milo, S. Shen-Orr, S. Itzkovitz, N. Kashtan, D. Chklovskii, and U. Alon, Science **298**, 824 (2002).
[5] E. Ravasz, A. L. Somera, D. A. Mongru, Z. N. Oltvai, and A.-L. Barabasi, Science **297**, 1551 (2002).
[6] C. Song, S. Havlin, and H. A. Makse, Nature (London) **433**, 392 (2005); Nat. Phys. **2**, 275 (2006).
[7] L. K. Gallos, C. Song, S. Havlin, and H. A. Makse, Proc. Natl. Acad. Sci. U.S.A. **104**, 7746 (2007).
[8] H. Yang, C. Yin, G. Zhu, and B. Li, Phys. Rev. E **77**, 045101(R) (2008).
[9] B. J. Kim, Phys. Rev. Lett. **93**, 168701 (2004).
[10] M. E. J. Newman, SIAM Rev. **45**, 167 (2003).
[11] C. Zhou and J. Kurths, Chaos **16**, 015104 (2006); K. Park, Y. Lai, and S. Gupte, *ibid.* **16**, 015105 (2006).
[12] V. Sood and P. Grassberger, Phys. Rev. Lett. **99**, 098701 (2007).
[13] L. D. F. Costa and G. Travieso, Phys. Rev. E **75**, 016102 (2007).
[14] A. S. Ribeiro, S. A. Kauffman, J. Lloyd-Price, B. Samuelsson, and J. E. S. Socolar, Phys. Rev. E **77**, 011901 (2008); P. Krawitz and I. Shmulevich, *ibid.* **76**, 036115 (2007).
[15] K.-I. Goh, B. Kahng, and D. Kim, Phys. Rev. E **64**, 051903 (2001); S. N. Dorogovtsev, A. V. Goltsev, J. F. F. Mendes, and A. N. Samukhin, *ibid.* **68**, 046109 (2003); C. P. Zhu, S. J. Xiong, Y. J. Tian, N. Li, and K. S. Jiang, Phys. Rev. Lett. **92**, 218702 (2004); C. Kamp and K. Christensen, Phys. Rev. E **71**, 041911 (2005); M. Sade, T. Kalisky, S. Havlin, and R. Berkovits, *ibid.* **72**, 066123 (2005); P. N. McGraw and M. Menzinger, *ibid.* **75**, 027104 (2007); J. N. Bandyopadhyay and S. Jalan, *ibid.* **76**, 026109 (2007).
[16] H. Yang, F. Zhao, L. Qi, and B. Hu, Phys. Rev. E **69**, 066104 (2004); F. Zhao, H. Yang, and B. Wang, *ibid.* **72**, 046119 (2005); H. Yang, F. Zhao, and B. Wang, Physica A **364**, 544 (2006); Chaos **16**, 043112 (2006).
[17] S. J. Xiong and S.N. Evangelou, Phys. Rev. B **52**, R13079 (1995); C. Zhu and S. J. Xiong, *ibid.* **62**, 14780 (2000); L. Gong and P. Tong, Phys. Rev. E **74**, 056103 (2006).
[18] J. Yi and B. J. Kim, Phys. Rev. B **76**, 245207 (2007).
[19] M. Dresselhaus, G. Dresselhaus, P. Eklund, and R. Saito, Phys. World **11**(1), 33 (1998); P. G. Collins and P. Avouris, Sci. Am. **283**, 62 (2000); R. H. Baughman, A. A. Zakhidov, and W. A.

de Heer, Science **297**, 787 (2002); G. Gruner, J. Math. Chem. **16**, 3533 (2006); Anal. Biochem. **384**, 322 (2006); Sci. Am. **17**, 48 (2007).
[20] E. Lopez, S. V. Buldyrev, S. Havlin, and H. E. Stanley, Phys. Rev. Lett. **94**, 248701 (2005); Z. Wu, L. A. Braunstein, S. Havlin, and H. E. Stanley, *ibid.* **96**, 148702 (2006); G. Li, L. Braunstein, S. Buldyrev, S. Havlin, and H. Stanley, Phys. Rev. E **75**, 045103(R) (2007).
[21] P. W. Anderson, Phys. Rev. **109**, 1492 (1958); P. A. Lee and T. V. Ramakrishnan, Rev. Mod. Phys. **57**, 287 (1985).
[22] Y.-J. Kim, M. H. Lee, and M. Y. Choi, Phys. Rev. B **40**, 2581 (1989).
[23] M. Titov and H. Schomerus, Phys. Rev. Lett. **91**, 176601 (2003).
[24] C. Tang and M. Kohmoto, Phys. Rev. B **34**, 2041 (1986).
[25] M. Kohmoto, B. Sutherland, and C. Tang, Phys. Rev. B **35**, 1020 (1987).
[26] M. Mezard, G. Parisi, and A. Zee, Nucl. Phys. B **559**, 689 (1999); S. Ciliberti, T. S. Grigera, V. Martin-Mayor, G. Parisi, and P. Verrocchio, Phys. Rev. B **71**, 153104 (2005).
[27] M. Sade and R. Berkovits, Phys. Rev. B **68**, 193102 (2003).
[28] E. L. Albuquerque and M. G. Cottam, Phys. Rep. **376**, 225 (2003).
[29] M. Janssen, Phys. Rep. **295**, 1 (1998).
[30] A. D. Mirlin, Phys. Rep. **326**, 259 (2000).
[31] J. Pipek and I. Varga, Phys. Rev. A **46**, 3148 (1992).
[32] I. Varga and J. Pipek, Phys. Rev. E **68**, 026202 (2003) and the references there-in.
[33] I. Varga, Phys. Rev. B **66**, 094201 (2002).
[34] T. Guhr, A. Muller-Groeling, and H. A. Weidenmuller, Phys. Rep. **299**, 189 (1998).
[35] T. Dittrich, Phys. Rep. **271**, 267 (1996).
[36] R. Berkovits and Y. Avishai, Phys. Rev. B **53**, R16125 (1996).
[37] B. L. Altshuler, I. Kh. Zharekeshev, S. A. Kotochigova, and B. I. Shklovskii, Zh. Eksp Teor. Fiz **94**, 343 (1988) [Sov. Phys. JETP **67**, 625 (1988)].
[38] B. I. Shklovskii, B. Shapiro, B. R. Sears, P. Lambrianides, and H. B. Shore, Phys. Rev. B **47**, 11487 (1993).
[39] E. Hofstetter and M. Schreiber, Phys. Rev. B **48**, 16979 (1993).
[40] M. L. Goldstein, S. A. Morris, and G. G. Yen, Eur. Phys. J. B **41**, 255 (2004); M. E. J. Newman, Contemp. Phys. **46**, 323 (2005); A. Clauset, C. R. Shalizi, and M. E. J. Newman, e-print arXiv:0706.1062v1.
[41] P. C. H. Ivanov, L. A. N. Amaral, A. L. Goldberger, S. Havlin, M. G. Rosenblum, Z. R. Struzik, and H. E. Stanley, Nature (London) **399**, 461 (1999).
[42] H. Jeong, B. Tombor, R. Albert, Z. N. Oltvai, and A.-L. Barabasi, Nature (London) **407**, 651 (2000).
[43] R. Overbeek *et al.*, Nucleic Acids Res. **28**, 123 (2000); see also http://igweb.integratedgenomics.com/IGwit
[44] Z. Liu and B. Li, Phys. Rev. E **76**, 051118 (2007).
[45] B. J. Kim, H. Hong, and M. Y. Choi, Phys. Rev. B **68**, 014304 (2003).
[46] S. Condamin, O. Benichou, V. Tejedor, R. Voituriez, and J. Klafter, Nature (London) **450**, 77 (2007).
[47] F. D. A. Aarao Reis, J. Phys. A **29**, 7803 (1996); C. Schulzky, A. Franz, and K. H. Hoffmann, ACM SIGSAM Bull. **34**, 1 (2000); A. Franz, C. Schulzky, S. Tarafdar, and K. H. Hoffmann, J. Phys. A **34**, 8751 (2001); D. H. N. Anh, K. H. Hoffmann, S. Seeger, and S. Tarafdar, Europhys. Lett. **70**, 109 (2005); D. H. N. Anh, P. Blaudeck, K. H. Hoffmann, J. Prehl, and S. Tarafdar, J. Phys. A **40**, 11453 (2007).